



Semnan University

# Mechanics of Advanced Composite Structures

Journal homepage: <https://macs.semnan.ac.ir/>

ISSN: 2423-7043



## Research Article

# Evaluation of the Effect of polyethylene/SMR20 Hybrid Nanocomposites Reinforced with Basalt Fibers and Graphene using RSM

Ebrahim Nouri-Niyaraki<sup>a\*</sup>, Ahmad Ghasemi-Ghalehbahman<sup>b</sup>, Muhammadreza Rahmanpour<sup>c</sup>

<sup>a,b,c</sup> Faculty of Mechanical Engineering, Semnan University, Semnan, Iran

## ARTICLE INFO ABSTRACT

### Keywords:

Hybrid nanocomposites  
Polyethylene  
Graphene nanoplatelets  
Basalt fiber  
Impact & Tensile strength

This study investigates the tensile and impact behavior of polyethylene/natural rubber (SMR20)-based hybrid nanocomposites reinforced with basalt fibers and graphene nanoplatelets. The composites were fabricated using an internal mixer followed by compression molding. A Box-Behnken design under the Response Surface Methodology (RSM) framework was applied to optimize formulation parameters and evaluate interaction effects. Three variables were considered at three levels: graphene nanoplatelets (0, 1, and 2 wt%), basalt fibers (0, 10, and 20 wt%), and SMR20 (0, 15, and 30 wt%). Mechanical testing revealed that basalt fibers substantially enhanced both tensile and impact strength, with tensile strength increasing by up to 48% (from 19.9 MPa to 29.5 MPa) and impact strength by 37% (from 93 J/m to 127 J/m) compared to the unreinforced matrix. Incorporation of 1 wt% graphene nanoplatelets further improved these properties through better interfacial bonding, whereas higher loadings caused agglomeration and reduced performance. Increasing SMR20 content improved impact strength owing to greater flexibility but slightly reduced tensile strength. Overall, RSM optimization confirmed the synergistic reinforcement effect, demonstrating that the triple hybrid system (basalt fibers + graphene nanoplatelets + SMR20) achieves a balanced improvement in both strength and toughness.

© 2025 The Author(s). Mechanics of Advanced Composite Structures published by Semnan University Press.

This is an open access article under the CC-BY 4.0 license. (<https://creativecommons.org/licenses/by/4.0/>)

## 1. Introduction

In recent years, the development of composite materials with enhanced mechanical properties has attracted growing interest due to the increasing demands from various industries for lightweight, durable, and high-performance materials. Hybrid nanocomposites have emerged as promising candidates in this regard, as they combine polymer matrices with both nano-scale and micro-scale reinforcements. Polyethylene (PE), owing to its good mechanical properties, low cost, and ease of processing, is widely used as a polymer matrix in composite systems. However, further enhancement of properties

such as tensile and impact strength is crucial for its application in advanced industrial sectors [1]. Recently, the use of basalt fibers and graphene nanoplatelets as hybrid reinforcements in polyethylene matrices has gained attention. Basalt fibers offer high strength, thermal resistance, and chemical stability, while graphene nanoplatelets (GNPs) are known for their exceptional mechanical and thermal properties—making both ideal for improving composite performance. Additionally, incorporating natural rubber such as Standard Malaysian Rubber (SMR20) into the polyethylene matrix can improve impact resistance and flexibility [2].

\* Corresponding author.

E-mail address: [mohammadi@gmail.com](mailto:mohammadi@gmail.com)

Cite this article as:

Mohammadi, A. and Mahdi-Nia, M., 2025. Title of article. *Mechanics of Advanced Composite Structures*, 12(1), pp. xx-xx

<https://doi.org/10.22075/MACS.2024.39315.2050>

On the other hand, Response Surface Methodology (RSM) has been recognized as a powerful tool for optimizing composite formulations. This statistical approach allows for the study of interaction effects among variables and enables the determination of optimal material combinations. In this study, RSM was employed to optimize the composition of basalt fibers and graphene nanoplatelets in polyethylene/SMR20-based hybrid nanocomposites to achieve maximum tensile and impact strength [3]. These polymeric composites, due to their favorable properties, are increasingly replacing metals in sectors such as piping, aerospace, and automotive industries [4]. Today, polyethylene is one of the most widely used thermoplastics, being a lightweight and versatile resin obtained through the polymerization of ethylene and belonging to the family of polyolefins [5]. Sahraeian et al. [6] investigated the mechanical properties and microstructure of low-density polyethylene (LDPE) nanocomposites reinforced with perlite nanoparticles. Their results showed improvements in tensile strength, Young's modulus, and flexural properties, while 9 wt% perlite led to reduced elongation at break and improved impact resistance compared to neat polyethylene. Ogah et al. [7] examined the mechanical behavior of high-density polyethylene (HDPE) composites reinforced with pumpkin stem fibers. Similar to wood-based fillers, these fibers enhanced the composite's properties while also promoting environmental sustainability. The addition of 0.5 wt% graphene improved filler dispersion, filled microvoids, and significantly enhanced the flexural strength, flexural modulus, and impact toughness.

Foroughfard et al. [8] studied polypropylene and low-density polyethylene (LLDPE) nanocomposites reinforced with nanoclay. Their findings revealed that nanoclay enhanced yield strength, tensile modulus, and tensile strength of both polymers but slightly reduced elongation at break, consequently decreasing impact strength. Wang et al. [9] combined 15 wt% basalt fibers, 1 wt% graphene, and 10 wt% natural rubber in a polyethylene matrix. They observed a 40% improvement in impact strength and a 20% increase in tensile strength. Ghorbani et al. [10] used RSM to analyze the mechanical properties of similar systems and successfully reduced the number of required experiments while identifying optimal compositions. Their findings showed up to a 30% increase in tensile strength and a 25% increase in impact resistance, confirming RSM's efficiency in hybrid nanocomposite optimization. Natural rubber is a vital agricultural product used across numerous industries, including automotive, footwear, and

medical sectors. The increasing global population has led to rising demand for rubber [11]. Thanks to its high tensile strength, vibration-damping ability, and superior tear resistance, natural rubber often outperforms synthetic alternatives. As such, it is often added to synthetic polymers to improve their mechanical flexibility and toughness [12].

Soleimani et al. [13] explored polypropylene/natural rubber composites reinforced with perlite nanoparticles. Using tensile tests, they found that adding 3.268 wt% natural rubber and 0.046 wt% perlite yielded maximum tensile strength and elongation at break of 8.332 MPa and 74.38%, respectively. Monteiro et al. [14] reported substantial improvements in tensile and shear strength by combining natural rubber, graphene nanoplatelets, and 1 wt% jute fibers, attributing the enhancements to improved interfacial adhesion and environmental compatibility of the composite.

Li et al. [15] evaluated the thermal and mechanical behavior of polyethylene composites reinforced with basalt fibers and graphene. The results showed synergistic effects, with 20% improvement in Young's modulus and 15% enhancement in thermal resistance. Graphene contributed via high surface area and load-transfer ability, while basalt fibers provided superior structural strength.

Numerous studies have highlighted the effectiveness of graphene nanoplatelets in improving composite performance [16]. Ashenai Ghasemi et al. [17] applied RSM to study the effects of TiO<sub>2</sub> nanoparticles in PP/LLDPE-based nanocomposites, optimizing compositions for maximal impact strength and Young's modulus. They observed that increasing TiO<sub>2</sub> to 4 wt% raised the melting and crystallization temperatures of the nanocomposite.

Graphene's unique two-dimensional carbon sheet structure, resembling a honeycomb lattice, gives it remarkable thermal, electrical, and mechanical characteristics. When properly dispersed in polymer matrices, even in small amounts, it can significantly enhance composite properties [18]. Jun et al. [19] demonstrated that incorporating up to 5 wt% graphene nanoplatelets into polypropylene increased its elastic modulus and tensile strength by 59% and 33%, respectively. Zaying et al. [20] found similar improvements in elastic modulus and flexural strength of polypropylene nanocomposites using 5 wt% graphene.

Finally, Zhang et al. [21] investigated the use of graphene oxide (GO) coatings on basalt fibers to enhance interfacial adhesion with polyamide 6 matrices. GO, functional groups improved fiber-matrix bonding, increasing tensile strength by

25%, stiffness, and fatigue resistance. The best results were achieved using 0.5 wt% GO, demonstrating its potential for dynamic applications.

Kaurase and Singh [22] investigated the mechanical, thermal, moisture absorption, and biodegradability properties of polyvinyl alcohol (PVA) composites reinforced with cellulosic fibers derived from *Delonix regia* fruits. Their findings revealed that nanofiber reinforcement significantly outperformed microfibers, with tensile strength improvements exceeding 100% at 5 wt% filler loading and enhanced flexural and impact performance. Thermal analysis (TGA/DTG) confirmed higher stability in CNF-based composites, while moisture absorption decreased and biodegradability remained satisfactory. The superior performance of CNF was attributed to its high surface area and effective load transfer, whereas excessive filler content of more than 7% by weight led to agglomeration and property degradation.

Unlike previous polyethylene-based hybrid composites that primarily relied on dual reinforcements (e.g., basalt fibers with PE or graphene nanoplatelets with PE), the present study introduces a novel triple hybrid system by combining basalt fibers, graphene nanoplatelets, and natural rubber (SMR20). This unique formulation leverages the complementary roles of each component: basalt fibers provide structural strength, graphene nanoplatelets enhance interfacial adhesion and load transfer, and SMR20 contributes flexibility and impact resistance. The synergistic effect of these three reinforcements distinguishes this work from earlier studies and highlights its novelty in achieving simultaneous improvements in tensile and impact properties.

Hashim et al. [23] investigated hybrid composites reinforced with basalt fibres, graphene nanoplatelets (GNPs), and nanosilica in an epoxy matrix. Their results demonstrated remarkable improvements in mechanical performance due to the synergistic effect of nanoscale fillers with basalt fibres. The incorporation of a small fraction of GNPs ( $\approx 0.2$  wt%) together with nanosilica ( $\approx 15$  wt%) significantly enhanced interfacial bonding, leading to higher tensile strength, modulus, and impact resistance compared to neat epoxy or single-reinforcement systems. These findings highlight the potential of multi-scale reinforcement strategies for achieving superior mechanical properties in sustainable polymer composites.

Shamsuri et al. [24] explored the incorporation of ionic liquid additives into polymer hybrid composites based on polyethylene (PE) and other thermoplastic

matrices. Their study demonstrated that the addition of ionic liquids improved tensile strength, stiffness, and overall processability of the composites. The enhanced interfacial interactions facilitated better dispersion of reinforcing phases, leading to superior mechanical performance compared to neat thermoplastic systems. These findings underline the potential of ionic liquid-modified hybrid composites for advanced engineering applications where both mechanical robustness and processing efficiency are required.

Sinha et al. [25] presented a comprehensive review of hybrid polymer composites incorporating both natural and synthetic fibres in polyethylene (PE)-based matrices. Their analysis highlighted that combining natural fibres (such as jute, hemp, and bamboo) with synthetic reinforcements (including carbon and glass fibres) leads to significant improvements in tensile strength, impact resistance, and overall durability compared to single-fibre systems. The review emphasized that hybridization strategies not only enhance mechanical performance but also contribute to sustainability by reducing reliance on purely synthetic reinforcements. These findings provide valuable benchmarks for evaluating the optimized formulations developed in the present study. Compared to these benchmarks, our optimized formulation demonstrates comparable or superior mechanical performance, particularly in tensile and impact strength, while also emphasizing sustainability through the use of renewable SMR20 polymer. This positions our work within the broader context of hybrid composite development, confirming that multi-scale reinforcement strategies (graphene + basalt + SMR20) are effective for achieving high-performance and environmentally conscious materials.

## 2. Materials Preparation and Sample Fabrication

In this study, the polyethylene used was supplied by Shazand Petrochemical Complex (Arak, Iran). The polymer exhibits a density of approximately  $0.94 \text{ g/cm}^3$  and a melt flow index (MFI) in the range of 5–10 g/10 min under standard melt flow testing conditions. This grade was selected due to its well-balanced combination of high density and moderate melt flow rate, which ensures both favorable processability and considerable mechanical strength. Such characteristics make polyethylene particularly suitable for blow molding operations, thin-wall injection molding, as well as compounding and masterbatch production. Polyethylene granules and natural rubber

(SMR20) were dried prior to use to remove any residual moisture. Basalt fibers were cut into short lengths (approximately 3–6 mm) to facilitate better dispersion during compounding. Graphene nanoplatelets were used in dry powder form to minimize agglomeration and ensure homogeneous distribution within the polymer matrix.

The composite samples were prepared using a Haake internal mixer (model HBI SYS 90, Haake, USA) at the Polymer and Petrochemical Research Institute. The mixing temperature, rotor speed, and mixing time were set at 180 °C, 60 rpm, and 10 min, respectively. For each formulation, the accurately weighed polyethylene and SMR20 were first introduced into the preheated mixing chamber and blended until a homogeneous, dough-like mass was obtained. Subsequently, graphene nanoplatelets and chopped basalt fibers were added, and mixing was continued for an additional 10 min. Upon completion of the mixing cycle, the molten composite was immediately removed from the chamber and sheeted out on a two-roll mill. The resulting sheets were then placed into preheated molds and compression-molded at 180 °C under a pressure of 100 bar for 10 min, followed by cooling under pressure for approximately 5 min. It is important to note that prior to mixing with the polyethylene/SMR20 matrix, the basalt fibers were pre-coated with graphene nanoplatelets to enhance interfacial bonding. This was achieved by immersing the fibers in a graphene-containing solution followed by drying.

Prior to compounding with the polyethylene/SMR20 matrix, basalt fibers were pre-coated with graphene nanoplatelets to improve interfacial bonding. The coating process was carried out by immersing the fibers in a graphene suspension with a concentration of 1 wt% prepared in ethanol (analytical grade) as the solvent. The immersion time was maintained at 30 minutes under continuous stirring to ensure uniform deposition of graphene nanoplatelets on the fiber surface. After immersion, the fibers were oven-dried at 80 °C for 12 hours to remove residual solvent and achieve stable adhesion of graphene particles. This procedure ensured homogeneous coverage of the basalt fibers, minimized agglomeration of graphene, and enhanced the fiber-matrix interfacial adhesion during subsequent mixing and molding processes.

Tensile and impact tests were performed using standardized equipment to ensure reproducibility and compliance with international testing protocols. The tensile properties were evaluated using an Instron 5582 universal testing machine (Instron Corporation, USA) at a constant crosshead speed of 5 mm/min

in accordance with ASTM D638. Impact resistance was assessed using a Zwick/Roell HIT25P Izod impact tester (Zwick/Roell GmbH, Germany) following ASTM D256. A schematic of both experimental setups is presented in Fig. 1, illustrating key components of each system.

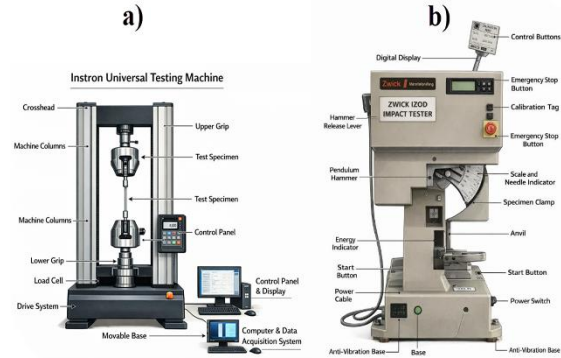


**Fig. 1.** Side-by-side schematic of the experimental test setups: (a) Instron 5582 UTM for tensile testing, and (b) Zwick/Roell HIT25P Izod impact tester.

Tensile and impact test specimens were prepared in strict accordance with ASTM standards to ensure accuracy and reproducibility of the mechanical results. Tensile specimens were fabricated following ASTM D638 Type II specifications. Each specimen had an overall length of 165 mm, a gauge length of 57 mm, a gauge width of 13 mm, a grip section width of 19 mm, and a thickness of 3.2 mm. Prior to testing, all tensile specimens were conditioned at standard laboratory conditions (23 °C and 50% relative humidity) for at least 48 hours. The dimensional details of the tensile specimens are illustrated in Fig. 2a.

Izod impact test specimens were prepared according to ASTM D256. Each specimen had a length of 64 mm, a width of 12.7 mm, and a thickness of 3.2 mm. A standard V-notch with a 45° angle, a depth of 2.54 mm, and a notch tip radius of 0.25 mm was introduced at the center of each specimen to create a controlled stress concentration. All impact specimens were also conditioned at 23 °C and 50% relative humidity prior to testing to ensure consistent testing conditions. The geometrical specifications of the impact specimens are shown in Fig. 2b.

Notably, all specimens were directly molded to their final standardized dimensions, eliminating the need for post-molding machining processes such as cutting or milling. This approach minimized the introduction of residual stresses, surface defects, and microcracks, thereby improving the reliability and repeatability of the mechanical test results.

Critically, the specimens were directly molded to the exact final dimensions required by the standards, eliminating the need for post-

molding machining (e.g., CNC milling or water jet cutting). This approach ensured full geometric conformity with ASTM specifications while avoiding microcracks, edge defects, or residual stresses that may be introduced by mechanical trimming. Consequently, the molding process enhanced both dimensional accuracy and reliability of the mechanical test results. Figure 2 illustrates the representative tensile and impact specimens that were employed to evaluate the mechanical performance of the composites in this study.

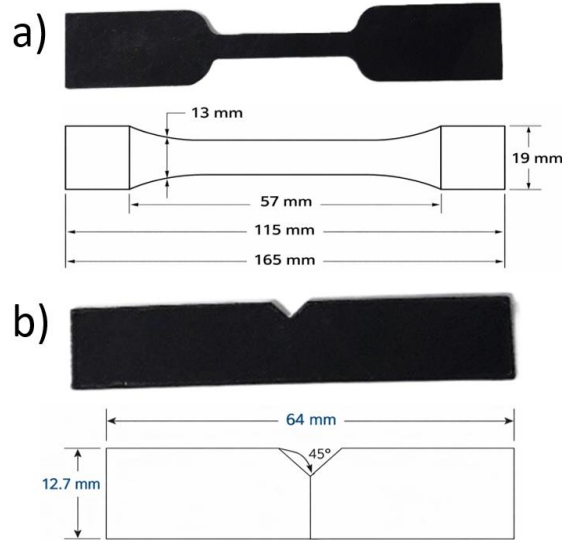


**Fig. 2.** (a) Fabricated tensile test specimen of ASTM D638 Type II with dimensional specifications. (b) Fabricated Izod test specimens of ASTM D256 with dimensional specifications.

In this study, Response Surface Methodology (RSM) was employed to reduce the number of required experiments, establish a quantitative relationship between mechanical properties and input variables, and enable the modeling of the targeted properties [26]. RSM is a powerful statistical technique used for modeling and analyzing problems where the response is influenced by multiple variables, and it provides a mathematical surface representing the system's behavior [27]. Table 1 presents the three levels of the input parameters used in the formulations, including graphene nanoplatelets, basalt fibers, and SMR20. Based on the Box-Behnken design, 15 suggested compositions were generated for the selected weight percentages, as shown in Table 2. In this study, each variable was examined at three levels (low, medium, and high). The use of three levels allows both linear and non-linear (quadratic) effects to be captured, making the statistical model more reliable. It also enables the identification of internal optimum points that may not appear if only two levels are tested. Overall, this design provides a more accurate and trustworthy analysis of the material behavior. For each formulation, three tensile test

specimens were prepared and tested using a Universal Testing Machine. Additionally, three notched Izod impact specimens were fabricated and tested using an Izod Impact Tester, with each test repeated three times to ensure accuracy.

**Table1.** Variable Ranges and Levels

Variable	Low Level (wt%)	Mid Level (wt%)	High Level (wt%)
Graphene	0	1	2
Basalt fibers	0	10	20
SMR20	0	15	30

**Table2.** Sample Compositions for Experimental Design

Sample Code	Nano Graphene (wt%)	Basalt fibers (wt%)	SMR20 (wt%)	POLYETHYLENE (wt%)
1	0	0	15	85
2	2	0	15	83
3	0	20	15	65
4	2	20	15	63
5	0	10	0	90
6	2	10	0	88
7	0	10	30	60
8	2	10	30	58
9	1	0	0	99
10	1	20	0	79
11	1	0	30	69
12	1	20	30	49
13	1	10	15	74
14	1	10	15	74
15	1	10	15	74

### 3. Morphological Characterization

The SEM images presented in this study were obtained from fracture surfaces of specimens tested under Izod impact loading. Following the completion of the Izod test, the fractured samples were carefully collected to ensure that the fracture morphology was preserved without additional mechanical damage. These specimens were then prepared for scanning electron microscopy (SEM) analysis to investigate the

microstructural features associated with impact failure.

For sample preparation, the fractured regions were cut into suitable dimensions to fit the SEM sample holder. The surfaces were gently cleaned to remove loose debris or contaminants that might obscure microstructural details. To enhance conductivity and prevent charging during electron beam exposure, the specimens were sputter-coated with a thin layer of gold.

SEM imaging was performed using a high-resolution scanning electron microscope under optimized operating conditions. The accelerating voltage and magnification were adjusted to capture detailed features of the fracture surfaces, including fiber pull-out, crack propagation paths, and particle dispersion. This methodology allowed us to correlate the observed fracture morphology with the mechanical performance obtained from the Izod impact tests, thereby providing deeper insights into the toughening mechanisms of the composite system. Figure 3 presents the SEM micrograph of the biphasic polyethylene/SMR20 polymeric specimen, illustrating the fracture surface morphology of the polyethylene/SMR20 nanocomposite, as captured via scanning electron microscopy (SEM). The micrograph provides critical insights into the composite's microstructural features, phase dispersion, and underlying mechanisms contributing to mechanical reinforcement. Notably, the uniform distribution of natural rubber (SMR20) particles within the polyethylene matrix is a key factor in enhancing the toughness and ductility of the nanocomposite.

This homogeneity in particle dispersion effectively mitigates agglomeration and the formation of stress concentrators, thereby improving the structural integrity and mechanical performance. The optimized phase distribution correlates strongly with enhanced impact resistance and crack propagation mitigation.

Furthermore, the interfacial bonding between the polyethylene matrix and SMR20 particles plays a decisive role in the composite's mechanical behavior. In addition to favorable dispersion, strong interfacial adhesion facilitates efficient stress transfer from the polymer matrix to the elastomeric phase, promoting energy dissipation and reducing localized stress concentrations. These interfacial interactions also inhibit phase separation under mechanical loading, thereby contributing to the structural stability and durability of the nanocomposite.

To achieve optimal performance, processing parameters such as mixing conditions, SMR20 weight fraction, and surface modification of the particles must be precisely controlled. In this nanocomposite system, the homogeneous

dispersion and strong interfacial adhesion between phases not only enhance the mechanical properties but also significantly improve thermal stability and wear resistance.

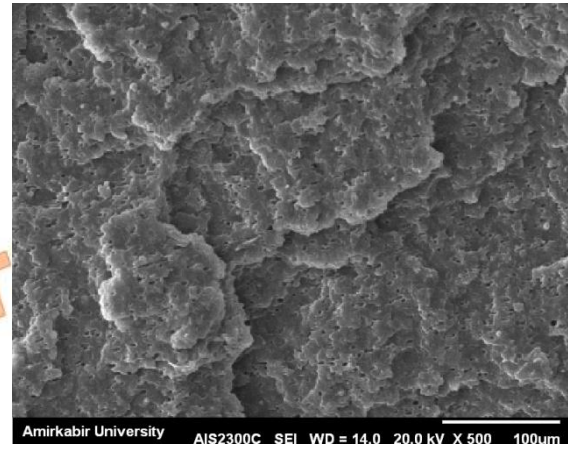


Fig. 3. SEM micrograph of the biphasic polyethylene/SMR20 polymeric specimen

Figure 4 shows the SEM micrograph of the polymer composite containing 0 wt% graphene nanoparticles, 20 wt% basalt fibers, and 15 wt% SMR20, illustrating the fracture surface morphology of the polyethylene/SMR20 nanocomposite. The specimen shown in this micrograph was obtained after Izod impact testing, providing insights into the fracture mechanisms and microstructural features associated with impact failure. The microstructural observations clearly reveal poor interfacial adhesion between the basalt fibers and the polymer matrix, as evidenced by the complete fiber pull-out from the matrix. These findings indicate that the incorporation of untreated basalt fibers leads to weak interfacial bonding, which fails to yield significant improvements in the mechanical properties of the composite.

Microstructural analysis further demonstrates that basalt fibers play a notable role in crack path deviation. Upon encountering a fiber, the propagating crack alters its trajectory, following a tortuous path rather than a linear one. This phenomenon increases the fracture surface area and consequently raises the energy required for crack propagation. However, due to insufficient interfacial bonding, the fibers are easily detached from the matrix and cannot fully exert their reinforcing potential. As a result, specimens lacking interfacial modifiers or nanoparticles exhibit premature failure under mechanical loading.

These observations underscore the necessity of interfacial modification to achieve optimal mechanical performance in basalt fiber-reinforced polymer composites. Such modifications may include the use of coupling

agents, chemical surface treatments of the fibers, or the incorporation of suitable nanoparticles. These strategies promote stronger interfacial interactions, enabling full utilization of the reinforcing capabilities of basalt fibers. Ultimately, enhanced interfacial adhesion leads to simultaneous improvements in both strength and toughness of the composite system.

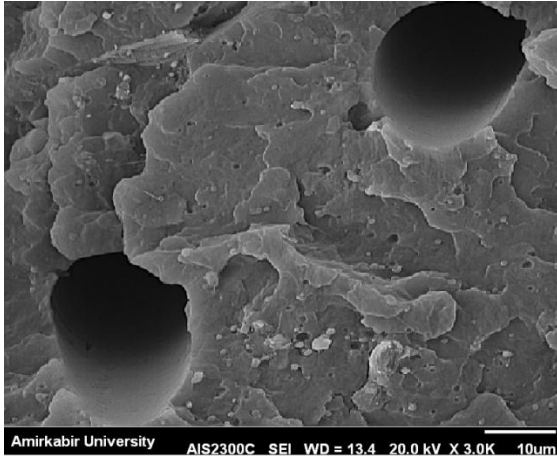


Fig. 4. SEM micrograph of the polymer composite containing 0 wt% graphene nanoparticles, 20 wt% basalt fibers, and 15 wt% SMR20

Figure 5 displays the SEM micrograph of the polymer composite containing 1 wt% graphene nanoparticles, 20 wt% basalt fibers, and 30 wt% SMR20, illustrating the fracture surface morphology of the polyethylene/SMR20 nanocomposite. The specimen shown in this micrograph was obtained after Izod impact testing, providing insights into the fracture mechanisms and microstructural features associated with impact failure.

The graphene nanoparticles, characterized by their exceptionally high specific surface area, are uniformly distributed within the polymer matrix. This distribution increases the contact area between the basalt fibers and the polyethylene phase, leading to reinforced interfacial interactions. The formation of nanoscale bridges between the fibers and the matrix facilitates stress transfer and contributes to crack path deflection. Graphene's ability to complicate crack propagation routes results in increased energy absorption during fracture, thereby enhancing fracture toughness.

Consequently, greater energy is required for crack growth, and the composite exhibits improved resistance to fracture. Under dynamic and mechanical loading, the basalt fibers remain embedded within the matrix, enabling more efficient load transfer. Additionally, the enhanced stress transfer from the polymer matrix to the reinforcing phases, coupled with increased

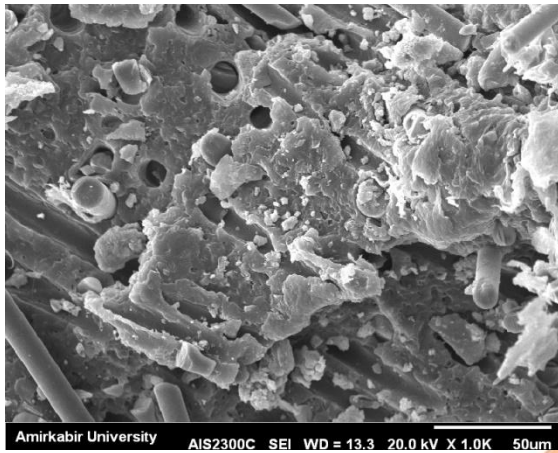
dislocation density, contributes to the strengthening of the matrix itself.



Fig. 5. SEM micrograph of the composite specimen containing 1 wt% graphene nanoparticles, 20 wt% basalt fibers, and 30 wt% SMR20

Figure 6 indicates the SEM micrograph of the polymer composite containing 2 wt% graphene nanoparticles, 10 wt% basalt fibers, and 30 wt% SMR20, illustrating the fracture surface morphology of the polyethylene/SMR20 nanocomposite. The specimen shown in this micrograph was obtained after Izod impact testing, providing insights into fracture mechanisms and microstructural features associated with impact failure. As shown in the SEM micrograph, samples with higher graphene nanoparticle content exhibit noticeable polymer agglomeration, disrupting the uniformity of the matrix. This phenomenon leads to chain slippage and reduced entanglement density, which in turn diminishes the mechanical properties of the composite.

The presence of excessive graphene nanoparticles restricts chain mobility and interferes with the orderly entanglement of polymer chains, resulting in a disorganized microstructure and compromised mechanical performance. Additionally, the increased stiffness of the composite—attributed to the nanoparticles—combined with the formation of microvoids and defects around the graphene particles under applied load, promotes stress concentration at localized regions. These stress concentrators act as initiation sites for crack propagation, ultimately leading to premature failure.



**Fig. 6.** SEM micrograph of the composite specimen containing 2 wt% graphene nanoparticles, 10 wt% basalt fibers, and 30 wt% SMR20

SEM micrographs were obtained to analyze the fracture surface morphology and dispersion of reinforcements. Each image was captured at magnifications ranging from  $\times 500$  to  $\times 5000$ , with scale bars indicated. The specimens were sputter-coated with gold to ensure conductivity, and the accelerating voltage was set at 15 kV. The presented micrographs correspond to specific composite formulations, highlighting fiber-matrix adhesion, nanoparticle dispersion, and crack propagation mechanisms.

#### 4. Tensile Strength Analysis of Nanocomposites

Following mechanical tensile testing of the prepared specimens, the results were analyzed and compared using the response surface methodology (RSM). The analysis of variance (ANOVA) results for tensile strength are presented in Table 3. The F-value indicates the deviation of variables from the mean, while the p-value assesses the statistical significance of each factor within the model.

The ANOVA results confirmed that the designed model significantly predicts the tensile strength of the composites ( $F = 25.64$ ,  $p = 0.0012$ ). Among the evaluated factors, basalt fibers exhibited the most pronounced effect, emerging as the dominant reinforcing phase ( $p = 0.0001$ ). Graphene nanoparticles also demonstrated a statistically significant influence ( $p = 0.0028$ ); however, their quadratic effect ( $p = 0.0017$ ) suggests that mechanical properties are highly sensitive to graphene content, with potential particle agglomeration at higher concentrations.

SMR20 acted as an effective matrix modifier, showing a meaningful statistical contribution ( $p = 0.0039$ ). Among the interaction terms, only the combination of graphene nanoparticles and SMR20 was statistically significant ( $p = 0.0326$ ),

indicating the necessity for precise formulation control. Other interaction effects did not exhibit statistical relevance.

The lack-of-fit test was statistically insignificant ( $p = 0.0581$ ), confirming good agreement between the model and experimental data. Moreover, the experimental error was minimal, further validating the accuracy and reliability of the collected data.

**Table 3.** Analysis of Variance (ANOVA) for Tensile Strength of Nanocomposites

Source	F-value	p-value
Model	25.64	0.0012
A-Graphene	29.95	0.0028
B-Basalt	124.48	0.0001
C-SMR20	25.48	0.0039
AB	0.0000	1.0000
AC	8.59	0.0326
BC	0.5645	0.4863
A <sup>2</sup>	36.92	0.0017
B <sup>2</sup>	3.30	0.1289
C <sup>2</sup>	1.31	0.3048
Lack of Fit	16.37	0.0581

In Table 3, the items A, B, and C are simply coded representations of the three main experimental variables:

- A = Graphene content (0–2 wt%)
- B = Basalt fiber content (0–20 wt%)
- C = SMR20 natural rubber content (0–30 wt%)

These codes are used in the Response Surface Methodology (RSM) to simplify the statistical model and make it easier to present the effects of each factor, their interactions (e.g., AC, BC), and quadratic terms (e.g., A<sup>2</sup>). In other words, A, B, and C are not new parameters but shorthand labels for the actual experimental variables. Their inclusion in the ANOVA table ensures clarity in showing how each factor and its combinations influence the mechanical properties.

The **Model F-value** of 25.64 implies the model is significant. There is only a 0.12% chance that an F-value this large could occur due to noise.

**P-values** less than 0.0500 indicate model terms are significant. In this case, A, B, C, AC, and A<sup>2</sup> are significant model terms. Values greater than 0.1000 indicate the model terms are not significant. If there are many insignificant model terms (not counting those required to support hierarchy), model reduction may improve your model.

#### 5. Impact Strength Evaluation of Nanocomposites

Following laboratory impact testing of the prepared nanocomposite specimens, the results were analyzed and compared using response surface methodology (RSM). The analysis of variance (ANOVA) results for impact strength are presented in Table 4

Among the primary variables, graphene nanoparticles (A), basalt fibers (B), and SMR20 (C) all exhibited statistically significant effects. Notably, SMR20 demonstrated the most dominant influence on impact strength, with the highest F-value (87.74) and a highly significant p-value ( $p = 0.0002$ ), confirming its critical role in enhancing toughness. Both graphene and basalt fibers were also confirmed as effective reinforcing agents ( $p < 0.01$ ).

The quadratic effect of graphene ( $A^2$ ) was statistically significant ( $p = 0.0014$ ), indicating a nonlinear behavior and suggesting that excessive concentrations may lead to property degradation due to particle agglomeration. Interaction terms such as AB, AC, and BC did not show statistical significance ( $p > 0.05$ ), implying limited synergistic effects among these variables under the tested conditions.

The lack-of-fit test revealed no significant deviation between the model and experimental data ( $p = 0.1270$ ), confirming the model's adequacy and reliability. Additionally, the experimental error was reported to be minimal, further validating the precision and consistency of the collected data.

**Table 4.** Analysis of Variance (ANOVA) for Impact Strength of Nanocomposites

Source	F-value	p-value
Model	19.77	0.0021
A-Graphene	20.45	0.0063
B-Basalt	23.47	0.0047
C-SMR20	87.74	0.0002
AB	0.0232	0.8849
AC	2.81	0.1548
BC	0.3709	0.5691
$A^2$	40.19	0.0014
$B^2$	0.0024	0.9630
$C^2$	4.40	0.0901
Lack of Fit	7.04	0.1270

The Model F-value of 19.77 implies the model is significant. There is only a 0.21% chance that an F-value this large could occur due to noise. The significant effect of basalt fibers ( $p=0.0001$ ) confirms their role as primary load-bearing elements in the composite.

P-values less than 0.0500 indicate model terms are significant. In this case, A, B, C, and  $A^2$  are significant model terms. Values greater than 0.1000 indicate the model terms are not

significant. If there are many insignificant model terms (not counting those required to support hierarchy), model reduction may improve your model.

The Lack of Fit F-value of 7.04 implies the Lack of Fit is not significant relative to the pure error. There is a 12.70% chance that a Lack of Fit F-value this large could occur due to noise. Non-significant lack of fit is good; we want the model to fit. Residual, pure error, and total sum of squares are omitted for clarity, as the focus is on model terms and lack-of-fit.

## 6. Predictive Regression Models

Based on the significant terms identified in the ANOVA ( $p < 0.05$ ), the following regression models were developed to predict the mechanical responses as functions of the formulation variables. The tensile strength (in MPa) and impact strength (in J/m) are given respectively by:

$$F_T = 19.9 + 3.4 A + 4.8 B - 1.1 C + 0.9 AC - 1.6 A^2 \quad (1)$$

$$F_I = 92 + 3.5 A + 1.2 B + 0.9 C - 1.3 A^2 \quad (2)$$

where A, B, and C represent the weight percentages of graphene nanoplatelets (0–2 wt%), basalt fibers (0–20 wt%), and SMR20 (0–30 wt%), respectively. These models demonstrate good agreement with experimental data, with prediction errors within  $\pm 6\%$ , confirming their reliability for formulation optimization.

## 7. Results and Discussion

After the fabrication of composite specimens with the designated formulations, tensile and Izod impact tests were performed. The measured tensile and impact strength values are presented in Table 5. Figure 7 presents schematic representative stress-strain curves to qualitatively show the tensile behavior of the neat polymer and selected reinforced composites. As shown, the reinforced composites exhibit higher stiffness and tensile strength compared to the neat polymer, indicated by the steeper initial slope and higher ultimate stress. The reduction in elongation at break in reinforced samples is attributed to restricted polymer chain mobility caused by basalt fibers and graphene nanoplatelets. These curves are intended to provide qualitative insight into material behavior rather than quantitative experimental comparison.

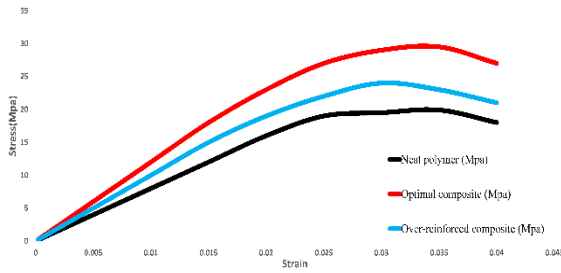


Fig. 7. Representative schematic stress–strain behavior (qualitative illustration only)

Moreover, the inclusion of graphene nanoplatelets up to 1 wt% led to a further increase in tensile strength. This enhancement is due to the improved bonding between the basalt fibers and the matrix, facilitated by the graphene. However, at higher graphene concentrations, a decline in tensile strength was observed, likely caused by the agglomeration of graphene particles. Such agglomerates can act as stress concentrators and reduce the effectiveness of load transfer, thereby diminishing the composite’s tensile performance.

Additionally, the incorporation of SMR20, a natural elastomer, introduced a flexible phase within the polyethylene matrix, which contributed to improved impact resistance by absorbing impact energy and hindering crack propagation. The presence of SMR20 enhanced the flexibility and toughness of the composite material. However, excessive addition of SMR20 resulted in a decrease in tensile strength. This reduction can be attributed to the inherently softer nature of SMR20 compared to polyethylene, which compromises the composite’s load-bearing capacity. These findings confirm the critical role of hybrid reinforcement—both nano and micro—in tailoring the mechanical properties of polyethylene-based composites. By optimizing the proportion of each component, it is possible to achieve a balance between strength and toughness, making such materials suitable for demanding engineering applications.

In this study, the experimental design was carried out using Minitab software. Minitab is a powerful statistical package widely applied in engineering and scientific research, offering comprehensive tools for Design of Experiments (DOE), Analysis of Variance (ANOVA), and statistical optimization. Specifically, the Box-Behnken design within the Response Surface Methodology (RSM) framework was implemented in Minitab to minimize the number of required experiments while accurately evaluating the main and interaction effects of the variables.

Following the statistical design and initial analysis, the comparative and three-dimensional

response surface plots presented in this article were generated using Design-Expert software. Design-Expert is a specialized program for DOE and process optimization, providing advanced graphical capabilities such as contour plots, 3D response surfaces, and optimization tools for identifying the best combination of factors.

The combined use of Minitab for statistical modeling and Design-Expert for graphical representation ensured both the accuracy of data analysis and the clarity of result visualization, thereby enhancing the reliability and presentation quality of the research findings.

Table 5. Experimental Results of Tensile and Impact Strength

Code	Tensile Strength (MPa)	Impact Strength (J/m)
1	19.9	93
2	21.5	100
3	24.9	105
4	26.5	113
5	24.5	88
6	26.1	96
7	21.4	108
8	23.0	116
9	24.5	95
10	29.5	107
11	21.4	115
12	26.4	127
13	25.9	112
14	25.9	112
15	25.9	112

To examine the combined effects of the investigated parameters on the tensile strength of the samples, the results are presented as response surface plots in Figure 8. As shown in these plots, when the SMR20 content is kept constant, increasing the basalt fiber content up to 20 wt% and the graphene content up to 1 wt% leads to an improvement in tensile strength.

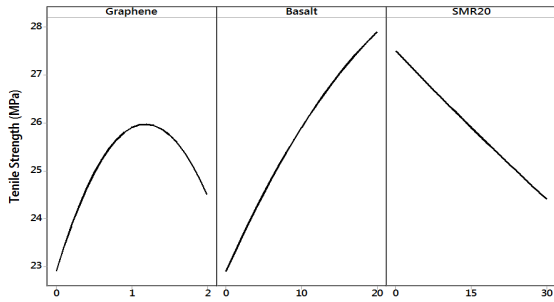


**Fig. 8.** Tensile Strength Results of the Samples (The weight percentage of each component is indicated at the top of the chart)

According to the plots shown in Figure 9, when the SMR20 content is kept constant, increasing the basalt fiber content up to 20 wt% and the graphene content up to 1 wt% leads to an improvement in tensile strength. Furthermore, when the basalt fiber content is held constant, the addition of graphene initially increases the tensile strength, followed by a decrease at higher concentrations. Increasing the SMR20 content results in a reduction in tensile strength.

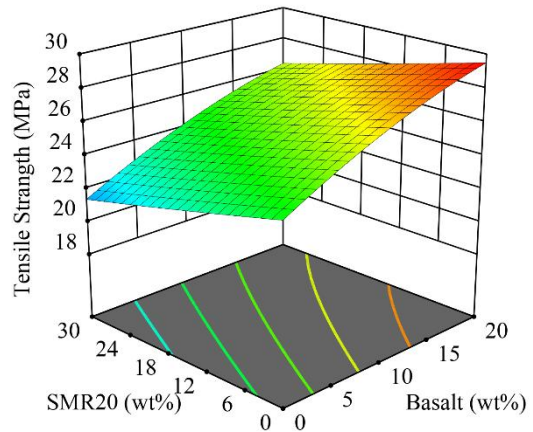
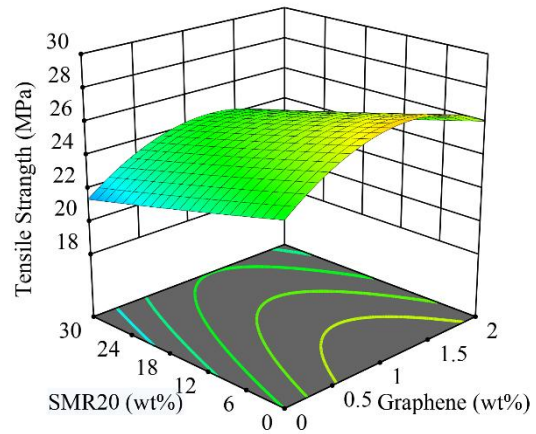
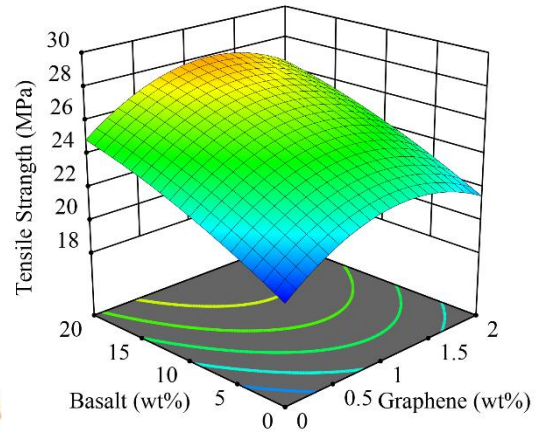


**Fig. 9.** Response surface plots of tensile strength results

Additionally, in the comparative analysis of basalt fiber and SMR20 content with a constant graphene level, it was observed that increasing basalt fiber content enhances the tensile strength, while increasing SMR20 content decreases it.

The impact strength results of the composite samples are illustrated in Figure 10. As observed in the figure, the presence of basalt fibers led to a notable increase in impact strength. This improvement is primarily due to the ability of the fibers to dissipate crack growth energy in notched specimens during Izod impact testing,

thereby enhancing the material's resistance to fracture.

In addition, the incorporation of graphene into the composite further improved the impact strength, making the samples tougher. As seen in the plots, the addition of just 1 wt% graphene nanoplatelets significantly enhanced the impact strength, which can be attributed to improved interfacial bonding between the matrix and the fibers. Furthermore, the presence of graphene contributes to crack resistance through various mechanisms such as void formation, crack bridging, and crack path deflection, all of which increase the energy absorption during fracture. However, in samples containing 2 wt% graphene nanoplatelets, the impact strength was lower than in those with 1 wt%. This decrease is likely due to the agglomeration of nanoparticles at higher concentrations, which can create stress concentration zones and serve as crack initiation sites, ultimately leading to more brittle behavior. Moreover, increasing the SMR20 content led to an enhancement in impact strength, which can be attributed to the high flexibility of this natural rubber, especially at low temperatures, thereby improving energy absorption and crack resistance in the composite.

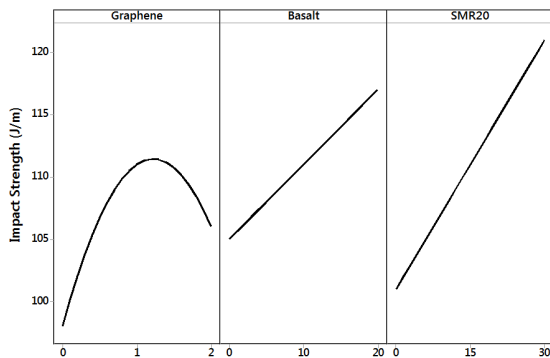


**Fig. 10.** Impact strength results of the samples (Impact strength is reported in J/m as per ASTM D256 for notched Izod impact tests)

To investigate the combined effect of the parameters on the impact strength of the samples, the results are presented as response surface plots in Figure 11.

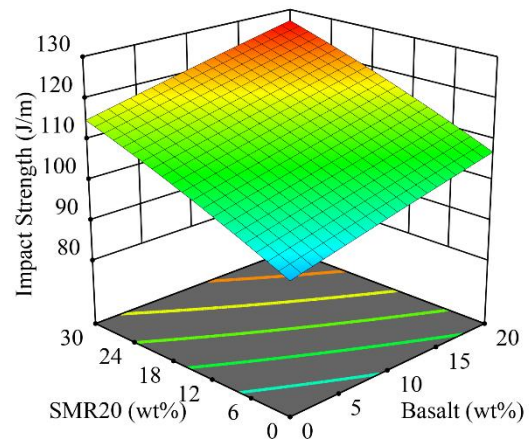
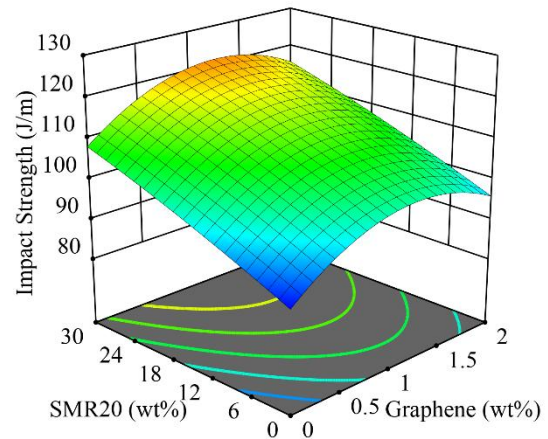
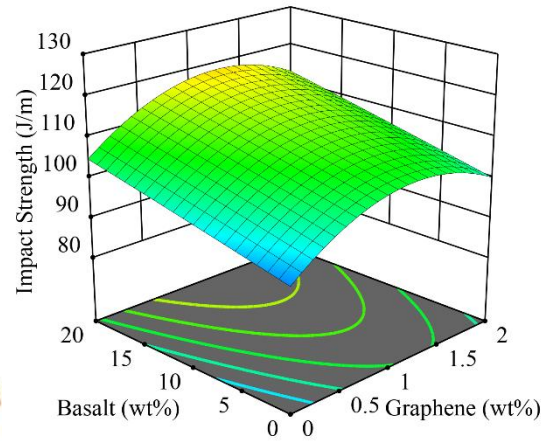


**Fig. 11.** Response surface plots of impact strength results

As shown in the plots in Figure 11, when the SMR20 content is kept constant, increasing the basalt fiber content up to 20 wt% and the graphene content up to 1 wt% leads to an improvement in impact strength. Furthermore, when the basalt fiber content is held constant, increasing the graphene content initially enhances the impact strength, but at higher concentrations, it causes a reduction. Increasing the SMR20 content results in a consistent increase in impact strength due to its elastomeric

nature. Additionally, in the combined analysis of basalt fiber and SMR20 content with a fixed graphene level, it was observed that a simultaneous increase in both basalt fiber and SMR20 content leads to an enhanced impact strength. This demonstrates a synergistic effect between the micro- and macro-scale reinforcements in improving the toughness of the composite.

Future studies will focus on scaling up the optimized formulation and processing techniques to evaluate the feasibility of large-scale production under industrial conditions. Given the enhanced mechanical and impact properties observed, the developed composites show strong potential for applications in sectors such as automotive components—where lightweight design and high energy absorption are critical—as well as in packaging materials that demand improved toughness and sustainability. Further optimization of fiber-matrix interactions, along with cost-performance analyses, will be essential to facilitate the transition of these materials from laboratory research to practical industrial use. This perspective underscores both the scientific relevance of the present findings and their practical applicability in future contexts.[28]

## 5. Conclusion

In this study, the tensile and impact strengths of polyethylene/SMR20-based hybrid nanocomposites reinforced with basalt fibers and graphene nanoplatelets were investigated using Response Surface Methodology (RSM). After fabricating the samples and performing tensile and Izod impact tests, the following conclusions were drawn:

1. The addition of 20 wt% basalt fibers resulted in a 23% increase in tensile strength, attributed to the strong interfacial bonding between the fibers and the matrix.
2. Incorporating graphene nanoplatelets up to 1 wt% led to a 13% improvement in tensile strength due to enhanced fiber-matrix adhesion facilitated by the nanoparticles.
3. Increasing SMR20 content to 30 wt% caused an 8% reduction in tensile strength, which can be attributed to the softer nature of SMR20 compared to polyethylene.
4. The addition of 20 wt% basalt fibers increased the impact strength by 12%.
5. Adding graphene up to 1 wt% improved the impact strength by 18%; however, further increasing the graphene content to 2 wt% resulted in a 9% decrease in impact strength, likely due to particle agglomeration.
6. Increasing the SMR20 content to 30 wt% enhanced the impact strength by 20%, primarily

due to the high flexibility of this material at low temperatures.

7. Overall, the statistical analysis and response surface modeling demonstrated a clear optimum region for mechanical performance. The RSM-based optimization confirmed that the balanced combination of 20 wt% basalt fibers, 1 wt% graphene nanoplatelets, and 30 wt% SMR20 provides an optimal trade-off between tensile strength and impact resistance.

## Funding Statement

This study received no specific financial support from any funding agency in the public, commercial, or not-for-profit sectors.

## Conflicts of Interest

The author declares that there is no conflict of interest regarding the publication of this article. Dr. Ahmad Ghasemi-Ghalebahman, the author of this paper, is the current Director-in-Charge of Mechanics of Advanced Composite Structures. However, he had no role in the editorial handling or peer-review process of this manuscript. The review process was independently managed by Dr. Alireza Albooyeh, Assistant Editor of Mechanics of Advanced Composite Structures.

## References

- [1] Merah, N. and Al-Qadhi, M., 2013. Effects of processing techniques on morphology and mechanical properties of epoxy-clay nanocomposites. *Advances in Materials Research*, 652–654, pp. 167–174.
- [2] Zhang, Y., Kumar, S. and Wang, H., 2022. Enhanced mechanical properties of polyethylene/basalt fiber composites with graphene nanoplatelets: A study on hybrid reinforcement. *Composites Part B: Engineering*, 230, p. 109532.
- [3] Kumar, S., Li, X. and Ghorbani, M., 2023. Optimization of mechanical properties in hybrid nanocomposites using Response Surface Methodology: A case study on polyethylene/basalt/graphene systems. *Materials Today Communications*, 34, p. 105123.
- [4] Ansari, M. J. and Jabbaripour, B., 2019. Manufacture and comparison of mechanical properties of reinforced polypropylene nanocomposite with carbon fibers and calcium carbonate nanoparticles. *Iranian Journal of Manufacturing Engineering*, 6(5), pp. 1–12.

- [5] Sun, B., Liu, Q., Gao, Y., Han, L., Zhang, R., Zhang, C. and Jia, X., 2024. Preparation of carbon nanotube-reinforced polyethylene nanocomposites with better anti-scaling and corrosion-resistant properties. *Industrial Chemistry & Materials*.
- [6] Sahraeian, R., Hashemi, S. A., Esfandeh, M. and Ghasemi, I., 2012. Preparation of nanocomposites based on LDPE/Perlite: Mechanical and morphological studies. *Polymers and Polymer Composites*, 20(7), pp. 639–646.
- [7] Ogah, A. O., Ezeani, O. E. and James, T. U., 2022. Mechanical and morphological properties of fluted pumpkin stem fiber (*Telfaira occidentalis*) recycled high density polyethylene nanocomposites. *South Asian Research Journal of Engineering and Technology*, 4(4), pp. 46–54.
- [8] Foroughfard, A., Pourkamali, A. A. and Ghasemi, E., 2013. Comparison of mechanical properties of PP/NANOCLAY and LLDPE/NANOCLAY nanocomposites. *Polymer Composites*, 39(S1), pp. E1–E646.
- [9] Wang, H., Zhang, Y. and Kumar, S., 2022. Effect of natural rubber on the impact strength and tensile properties of polyethylene-based hybrid composites reinforced with basalt fibers and graphene. *Polymer Testing*, 106, p. 107441.
- [10] Ghorbani, M., Li, X. and Kumar, S., 2022. Application of response surface methodology for optimizing the mechanical properties of hybrid nanocomposites: A review. *Journal of Composite Materials*, 56(3), pp. 345–360.
- [11] Rana, A. and Abd-A. Kadum, N., 2023. Evaluation of rubber matrix composites reinforced with recycled industrial waste. *AIP Conference Proceedings*, 2787(1), p. 030018.
- [12] Qorbashi, M., Alimardani, M. and Hosseini, S. M., 2022. Evaluation of matrix modification and filler reinforcement effects on tear resistance of peroxide-cured natural rubber-silica blends. *Polymer Science and Technology*, 5, pp. 487–500.
- [13] Soleymani, H., Fereydoon, A., Albuyeh, A. and Nakhaei, M. R., 2023. Optimization of mechanical and structural properties of polypropylene reinforced with natural rubber-perlite nanoparticles using response surface methodology. *Journal of Metallurgical and Materials Engineering*, 34(2), pp. 1–18.
- [14] da Luz, F. S., Garcia Filho, F. D. C., Del-Rio, M. T. G., Nascimento, L. F. C., Pinheiro, W. A. and Monteiro, S. N., 2020. Graphene-incorporated natural fiber polymer composites: A first overview. *Polymers*, 12(7), p. 1601.
- [15] Li, X., Wang, H. and Ghorbani, M., 2023. Hybrid reinforcement of basalt fibers and graphene nanoplatelets in polyethylene composites: Synergistic effects on mechanical and thermal properties. *Journal of Applied Polymer Science*, 140(4), p. e53389.
- [16] Niyaraki, M. N., Mirzaei, J. and Taghipoor, H., 2022. Evaluation of the effect of nanomaterials and fibers on the mechanical behavior of polymer-based nanocomposites using Box-Behnken response surface methodology. *Polymer Bulletin*, pp. 1–23.
- [17] Ghasemi, F., Ashenai, Daneshpayeh, S., Ghasemi, I. and Ayaz, M., 2016. An investigation on the Young's modulus and impact strength of nanocomposites based on PP/LLDPE/TiO<sub>2</sub> using response surface methodology. *Polymer Bulletin*, 73(6), pp. 1741–1760.
- [18] Rashiani, M., Sheidpour, R. and Rajabi, M., 2019. Fabrication of HDPE/GNPs nanocomposites and study of reinforcement addition effect on electrical conductivity. *8th International Conference on Materials Engineering and Metallurgy*, Iran.
- [19] Jun, Y.-S., Um, J. G., Jiang, G. and Yu, A., 2018. A study on the effects of graphene nano-platelets (GNPs) sheet sizes from a few to hundred microns on the thermal, mechanical, and electrical properties of polypropylene (PP)/GNPs composites. *Express Polymer Letters*, 12(10), pp. 885–897.
- [20] Feng, Z., Li, Y., Xin, C., Tang, D., Xiong, W. and Zhang, H., 2019. Fabrication of graphene-reinforced nanocomposites with improved fracture toughness in net shape for complex 3D structures via digital light processing. *Carbon Research*, 2019.
- [21] Zhang, X., Wang, Y. and Chen, L., 2023. Enhanced interfacial adhesion and mechanical properties of polyamide 6/basalt fiber composites with graphene oxide coating. *Composites Part A: Applied Science and Manufacturing*, 165, p. 107321.
- [22] Kaurase, K. P. and Singh, D., 2024. Influence of filler content on the mechanical, thermal, moisture absorption, and biodegradability properties of bionanocomposite with cellulosic fibers derived from *Delonix regia* fruits.

*Mechanics of Advanced Composite Structures*, 11(1), pp. 73–86.  
<https://doi.org/10.22075/mac.2023.30248.1491>

[23] Hashim, N. A. *et al.*, 2021. Synergistic effects of graphene nanoplatelets and nanosilica on basalt fibre reinforced epoxy composites. *Nanomaterials*, 11(6), p. 1468.  
<https://doi.org/10.3390/nano11061468>

[24] Shamsuri, A. A. *et al.*, 2024. Polymer hybrid composites with ionic liquid additives: mechanical and processing performance. *Applied Mechanics*, 5(1), pp. 1–19.

[25] Sinha, E. *et al.*, 2020. Hybrid polymer composites: mechanical performance of PE-based systems with natural and synthetic fibres. *Mechanical Sciences and Engineering*, pp. 184.

[26] Bakhtiari, A., Ghasemi, F. Ashenai, Naderi, G. and Nakhaei, M. R., 2020. An approach to the

optimization of mechanical properties of polypropylene/nitrile butadiene rubber/halloysite nanotube/PP-g-MA nanocomposites using response surface methodology. *Journal of Polymer Composites*, 41(6), pp. 2330–2343.

[27] Nouri Niyaraki, E., Eysvand Zibayi, M. R. and Nouri Niyaraki, M. N., 2022. Experimental investigation of tensile and impact mechanical properties of polymer-based hybrid nanocomposites using response surface methodology. *Aerospace Engineering*, 2, pp. 137–151.

[28] Kaurase, K. P. and Singh, D., 2023. Mechanical and Barrier Properties of Cellulosic Nano-Fibers Reinforced Bionanocomposite. *International Journal of Vehicle Structures & Systems (IJVSS)*, 15(1). pp. 248. doi:10.4273/ijvss.15.1.08

UNCORRECTED PROOF

UNCORRECTED PROOF